Algebraic approach to the structure of the low-lying states in $A \approx 100$ Ru isotopes

S. Kisyov,[1,2,*] D. Bucurescu,[2] J. Jolie,[3] and S. Lalkovski[1,†]

[1]*Faculty of Physics, University of Sofia "St. Kliment Ohridski," 1164 Sofia, Bulgaria*

[2]*Horia Hulubei National Institute for R&D in Physics and Nuclear Engineering (IFIN-HH), P.O. Box MG-6, Bucharest-Magurele, Romania*

[3]*IKP, University of Cologne, Zülpicher Strasse 77, D-50937 Köln, Germany*

(Received 15 February 2016; published 12 April 2016)

The structure of the low-lying states in the odd- and even-mass $A \approx 100$ Ru isotopes is studied in the framework of two algebraic models. The even-mass Ru nuclei are first described within the interacting boson model 1 (IBM-1). The output of these calculations was then used to calculate the odd-A isotopes within the interacting boson-fermion model 1 (IBFM-1), where a coupling of the odd neutron to the even-even core is considered. The level energies and transition probabilities calculated in the present work are tested against the experimental data. One-nucleon transfer spectroscopic factors as well as electromagnetic moments were also calculated for the odd-A Ru and compared to the experimental values. The transitional character of the isotopes is studied. Most of the low-lying positive-parity states in the odd-A Ru nuclei below 2 MeV are interpreted on the basis of $\nu d_{5/2}$ and $\nu g_{7/2}$ configurations. The role of the $\nu s_{1/2}$ orbital in the nuclear structure of the odd-mass Ru nuclei at low energies is also studied. The negative-parity states are interpreted as $\nu h_{11/2}$ excitations coupled to the core. The evolution of the IBM-1 and IBFM-1 parameters is discussed.

DOI: 10.1103/PhysRevC.93.044308

I. INTRODUCTION

The interplay between the collective and single-particle degrees of freedom is one of the major topics in nuclear physics. In many cases collective behavior develops quickly away from the closed shells, leading to deformed shapes. The evolution towards stable deformation in the ground state is preceded by transitional regions that are often challenging for theoretical description.

The $A \approx 100$ Ru isotopes are placed in such a region where a large variety of phenomena is present. They have six protons less and few neutrons more than the $Z = 50$ and $N = 50$ magic numbers, respectively, and hence are situated between the shell closures and the midshell area. The evolution of collective behavior in the even Ru nuclei can be traced in an explicit way, given that the energy of the 2_1^+ state and the $R_{4/2}$ ratio are sensitive to the degree of collectivity [1]. The energy of the first 2^+ states decreases and the $R_{4/2}$ ratio increases smoothly with raising neutron number. The absolute and relative electromagnetic transition probabilities also have a systematic behavior and indicate gradual changes in the nuclear structure towards heavier isotopes [2–6].

The even-A Ru were previously studied using various theoretical approaches. Taking into account the expected shape changes, the interacting boson model (IBM) [7,8] was found to reproduce accurately the properties of the even-even nuclei in this mass region. The model was applied with success to the Ru isotopes close to the line of β stability [9–17]. Calculations performed in the framework of the original version of the IBM-1 were used to interpret the structural change as a transition between the U(5) and O(6) limits of the IBM [10]. An adequate reproduction of the properties of the even Ru was also obtained using the N_pN_n parametrization [11] and the extended consistent-Q formalism (ECQF) in IBM-1 [12]. The IBM-2 version, treating the protons and neutrons independently, also gives a good description of the experimental characteristics [9].

The level schemes of the odd-A Ru nuclei, however, are more complex. The coupling of only one particle to the semimagic ^{94}Ru core leads to a number of states in ^{95}Ru, some of which having a prominent single-particle nature. The evolution of these states can be tracked towards the heavier isotopes. Other low-lying states seem to have more complex structure involving seniority $\nu = 3$ configurations [18].

Several studies of the odd-A Ru were performed within the interacting boson-fermion model (IBFM) [19,20] that includes coupling of the odd nucleon to an IBM core [21]. A wide systematic IBFM approach was based on IBM-2 calculated even-even Ru and a separate treatment of the boson-fermion interaction for the negative- and positive-parity states [22,23].

In the present work, spectroscopic data for $^{99-105}$Ru were interpreted within the IBFM-1 model. The even-even cores were calculated using the ECQF extension to IBM-1 and the properties of the odd-A Ru nuclei were calculated with the same set of boson-fermion interaction parameters for both positive- and negative-parity states and all the isotopes.

II. THE INTERACTING BOSON MODEL-1 (IBM-1)

The interacting boson model is widely used to describe the characteristics of even-even nuclei. Although based on relatively simple approximations, IBM is a powerful tool to explore the collective properties [24,25]. The basic model assumption is that nucleon pairs can be represented by interacting s and d bosons that have angular momenta $\ell = 0$ and $\ell = 2$, respectively. The number of interacting bosons is determined by the number of valence particles or holes relative

*stanimir.kisyov@phys.uni-sofia.bg

†Present address: Department of Physics, University of Surrey, Guildford, Surrey GU2 7XH, United Kingdom.

to the nearest shell closure. In the original IBM-1 version the proton and neutron degrees of freedom are not distinguished, in contrast to the IBM-2 extension, where they are separated.

Various representations of the IBM Hamiltonian exist and operators for several experimental observables can be constructed in terms of the boson creation and annihilation operators. The Hamiltonian and the operators describing electromagnetic transitions can be completely represented by using the $s,s^\dagger,\tilde{d},d^\dagger$ operators, where $\tilde{d}$ is a tensor operator defined by [24,25]

$$\tilde{d}_\mu = (-1)^\mu d_{-\mu}. \quad (1)$$

The model Hamiltonian is commonly used in the *multipole expansion* form [24],

$$H = \varepsilon n_d - \kappa' L^2 + \kappa'' P^\dagger P - \kappa Q^2 + a_3 T_3^2 + a_4 T_4^2, \quad (2)$$

where

$$\begin{aligned} n_d &= \sqrt{5}T_0, \quad L = \sqrt{10}T_1, \\ P &= \frac{1}{2}(\tilde{d}^{\,2} - s^2), \\ Q &= (d^\dagger s + s^\dagger \tilde{d}) + \chi (d^\dagger \tilde{d})^{(2)} = (d^\dagger s + s^\dagger \tilde{d}) + \chi T_2, \\ T_l &= (d^\dagger \tilde{d})^{(l)}, \quad l = 0,1,2,3,4. \end{aligned} \quad (3)$$

In this form the Hamiltonian has an operator for the number of d bosons, an angular momentum operator, a pairing operator, a quadrupole operator, and an octupole and hexadecapole terms [24].

The explicit form of the electromagnetic transition operator for $E2$ transitions is

$$T(E2) = e_B[(s^\dagger \tilde{d} + d^\dagger s) + \chi (d^\dagger \tilde{d})^{(2)}] = e_B Q, \quad (4)$$

where e_B denotes the effective boson charge.

The original version of IBM treats χ in the Hamiltonian as a constant ($\chi = -\sqrt{7}/2$), while χ in the $E2$ transition operator is a free parameter [26]. A reduction of the number of free parameters is achieved within the *consistent-Q formalism* (CQF) approach, where the model Hamiltonian is [27]

$$H = -\kappa Q^2 - \kappa' L^2. \quad (5)$$

In this approach the same value for χ is used to construct the Hamiltonian and the $E2$ transition operator. The CQF has been remarkably successful in describing the regions where deformed rotor to γ-soft shape transition takes place [27].

IBM is capable of reproducing not only the three limit cases, the anharmonic vibrator, deformed rotor, and γ-soft nucleus but also the transitions between them. That makes the model applicable for a wide range of nuclei [1,24,28,29].

III. EVEN-A Ru ISOTOPES

The IBFM-1 approach to the odd-A nuclei assumes the coupling of the odd particle to an even-even core described in the framework of IBM-1. Hence, calculations of the properties of the even $^{98-108}$Ru were first performed in the present work. The extended consistent-Q formalism (ECQF) approach was used as described in Ref. [12].

In the ECQF [30], the εn_d term is added to the basic CQF Hamiltonian. This is required by the major role that it has in the vibrational limit of the IBM:

$$H = \varepsilon n_d - \kappa Q^2 - \kappa' L^2. \quad (6)$$

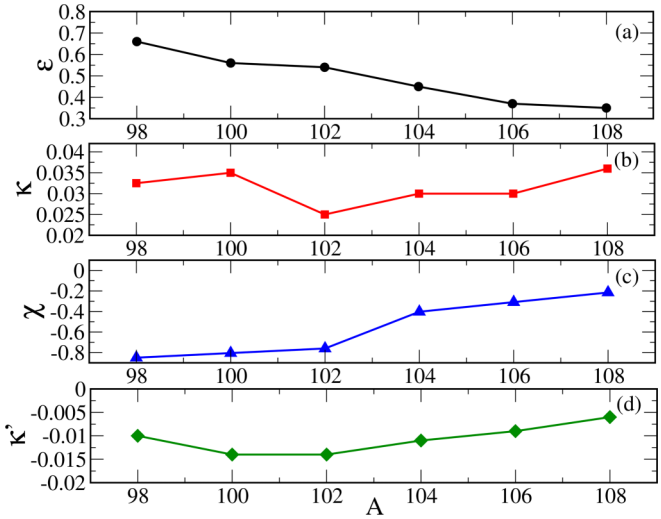

FIG. 1. Evolution of the IBM-1 parameters used in the present calculations. The changes are noted for (a) ε; (b) κ; (c) χ; (d) κ'.

Having this form of the Hamiltonian, the wave functions for a given boson number depend on the ε/κ and χ parameters. The κ and κ' parameters can be determined from a fit to the nuclear level energies.

The properties of the even $^{98-108}$Ru were calculated by using the PHINT program package [31]. The parameters included in the ECQF calculations are presented in Fig. 1. Their values were chosen to fit both the level energies and the $B(E2)$ values in the even Ru nuclei. A smooth behavior is observed for most of them. The ε parameter gradually decreases with increasing neutron number. This is related to the systematical downsloping trend of the energy of the first excited 2^+ state and the dominant role of the vibrational degrees of freedom near the closed shells. The χ parameter also exhibits a smooth behavior. In the present calculations it increases away from the $N = 50$ shell closure and approaches values close to 0 in the heavier isotopes. This is consistent with possible evolution of the structure towards the O(6) limit of IBM, related to the Wilets-Jean γ-unstable scheme [32].

A. Level schemes

The energies of the low-lying states in the ground, quasi-β, and quasi-γ bands give important information about the evolution of the collectivity in the isotopic chain.

A comparison between the experimental and IBM-1 calculated energies of the states in the ground-state bands is presented in Fig. 2. The 2_1^+ and 4_1^+ states in ^{98}Ru define a ratio $R_{4/2} = 2.14$. The $R_{4/2}$ value typical for the vibrational limit is 2 and hence ^{98}Ru has nearly vibrational structure. This is supported by the almost equidistant level energies of the first few states in the ground-state band. In the heavier Ru isotopes the first 2^+ level energy decreases and the $R_{4/2}$ ratio increases, reaching a value of 2.75 in ^{108}Ru.

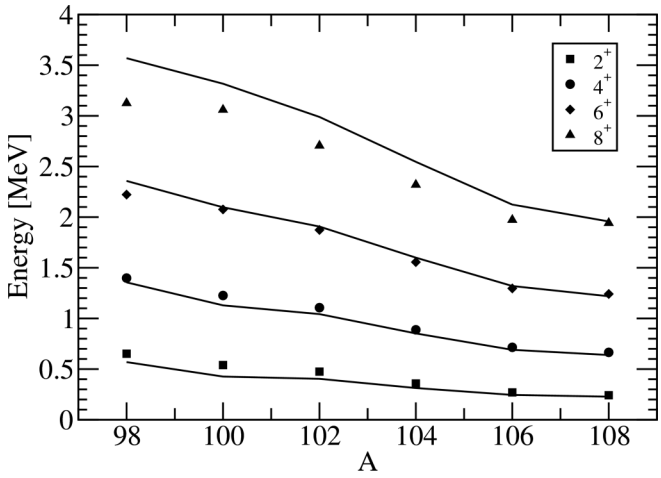

FIG. 2. Experimental (symbols) and calculated (lines) level energies in the ground-state bands in $^{98-108}$Ru. The experimental data are taken from Ref. [3].

The calculated energies of the states in the quasi-β and quasi-γ bands are compared to the experimental data in Fig. 3. $^{98-108}$Ru are placed in a transitional region where an onset of deformation is observed. In the vibrational limit the second 0^+ state is a member of the 0^+, 2^+, 4^+ triplet corresponding to the two-phonon excitation. In the Ru chain the 0_2^+ energy decreases with the neutron number up to $N = 58$. Then $E_{0_2^+}$ stays constant when adding more neutrons. This leads to splitting of the multiplet in the heavier isotopes and the 0_2^+ is separated from the 4_1^+ state of the ground-state band which decreases gradually in energy. This decoupling of the 0_2^+ from 4_1^+ state is a fingerprint of a deviation from the vibrational limit.

Within the Wilets-Jean model only the doublet 2^+, 4^+ is present, while the 0_2^+ state is placed at higher excitation energy [32,34]. Thus, an evolution towards γ-unstable nuclei is a

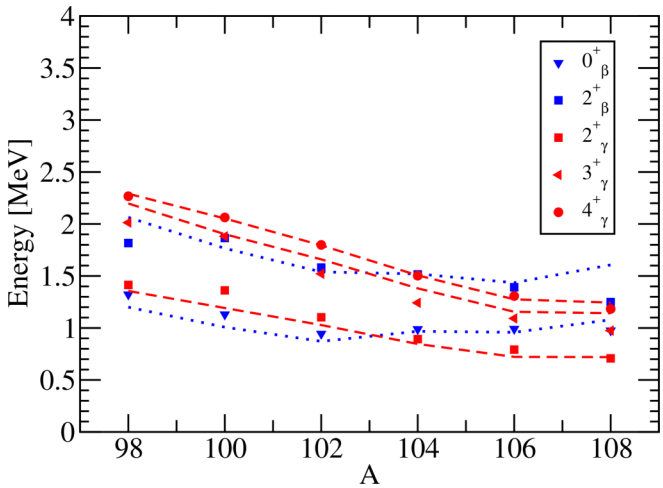

FIG. 3. Experimental and calculated level energies in the quasi-β and quasi-γ bands in $^{98-108}$Ru. The experimental energies of the states are noted with symbols. The dotted blue lines denote the IBM-1 predictions for the 0^+ and 2^+ states in the quasi-β bands. The theoretical energies of the states in the quasi-γ bands are shown with dashed red lines. The experimental data are taken from Refs. [3,33].

TABLE I. Experimental and calculated energy staggering indices $S(4,3,2)$ for $^{98-108}$Ru. $S(4,3,2)_{\rm exp}$ are calculated using data from Ref. [3].

Isotope	$S(4,3,2)_{\rm exp}$	$S(4,3,2)_{\rm IBFM}$
^{98}Ru	− 0.53	− 1.31
^{100}Ru	− 0.63	− 1.31
^{102}Ru	− 0.30	− 1.23
^{104}Ru	− 0.25	− 1.31
^{106}Ru	− 0.31	− 1.28
^{108}Ru	− 0.24	− 1.40

possible explanation of the 0_2^+ behavior. Approaching the O(6) limit the 0_2^+ state becomes the head of the quasi-β band. In the present calculations the 2_3^+ state which is a part of this band is also reproduced correctly.

The 2_2^+ state develops as the bandhead of a $\Delta J = 1$ quasi-γ band and its evolution can be traced in close relation to the behavior of the 4_1^+ state. Both levels are close in energy in all nuclei of this isotopic chain and are well described by the calculations.

The arrangement of the states in the quasi-γ bands gives strong arguments for the type of the axial asymmetry in the nuclei, if present. In the framework of the rigid triaxial rotor model the 3_γ^+ member of the band is placed close to the 2_γ^+ state, while in γ-soft nuclei 3_γ^+ and 4_γ^+ are nearly degenerate. In the present calculations the energies of the 3_γ^+ states are somewhat overestimated, but their general evolution pattern is reproduced. The 3_γ^+ states lie closer to the 4_γ^+ than to the 2_γ^+ states, suggesting that the nuclei of interest can be related to γ-soft behavior.

The energy staggering index

$$S(4,3,2) = \frac{(E_{4_\gamma^+} - E_{3_\gamma^+}) - (E_{3_\gamma^+} - E_{2_\gamma^+})}{E_{2_1^+}} \qquad (7)$$

is often used to discriminate different types of axial asymmetry. Thus, for example, values of the staggering index above 1/3 are typical for γ-rigid configurations, while $S(4,3,2) = -2$ corresponds to the γ-unstable case [1]. The experimental and calculated values for the staggering indices $S(4,3,2)$ in $^{98-108}$Ru are compared in Table I. The experimental data are reproduced in sign but not in magnitude.

B. Electromagnetic transition probabilities

More detailed information about the structural changes can be obtained by studying the transitions within and between the ground-state, quasi-β, and quasi-γ bands. Most of the $B(E2)$ values for the first few transitions in the even $^{98-108}$Ru ground-state bands are known. Data are also available for some of the transitions connecting the ground-state bands to the quasi-γ bands [3].

A comparison with the calculations is made for several low-lying $E2$ transitions. The $B(E2)$ values were calculated using the form of the $E2$ transition operator from Eq. (4) and the relation

$$B(\sigma L; J_i \to J_f) = \frac{1}{2J_i + 1} \langle J_f \| T(\sigma L) \| J_i \rangle^2, \qquad (8)$$

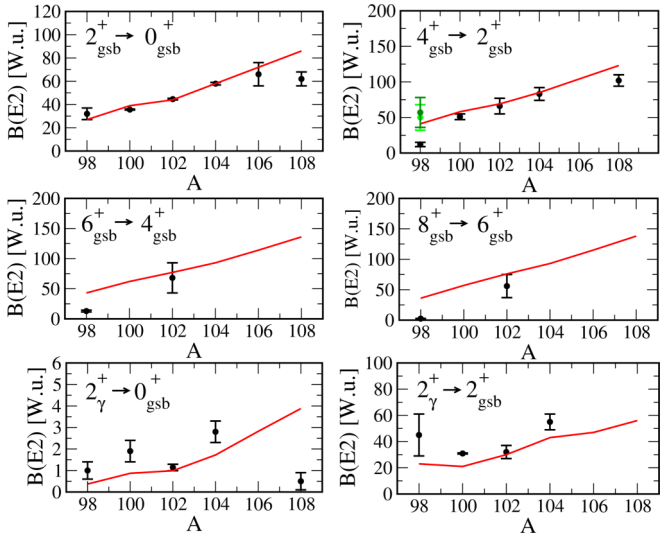

FIG. 4. IBM-1 absolute $B(E2)$ values (lines) and experimental data (symbols) for transitions in the even $^{98-108}$Ru. The experimental data are taken from Ref. [3] unless otherwise noted in the text.

where σ and L denote the type and the multipolarity of the transitions and J_i and J_f are the spins of the initial and final states.

A value of 0.100 eb was set for the effective boson charge e_B, chosen such as to fit the $B(E2)$ value for the $2^+_1 \rightarrow 0^+_1$ transition in ^{102}Ru. A comparison between the calculated transition probabilities and the available experimental data is presented in Fig. 4. The behavior of the calculated values is smooth and follows the overall trends of the experimental points, with the exception of the $2^+_{gsb} \rightarrow 0^+_{gsb}$ and $2^+_{\gamma} \rightarrow 0^+_{gsb}$ transitions in ^{108}Ru.

A notable difference with the evaluated data in Ref. [3] is observed for the $B(E2; 4^+_{gsb} \rightarrow 2^+_{gsb})$ in ^{98}Ru. The small experimental value adopted for the $B(E2; 4^+_{gsb} \rightarrow 2^+_{gsb})$ is related to the half-life of 7.6 (16) ps of the 4^+_1 state measured using the recoil-distance Doppler shift (RDDS) method [35]. The anomalous character of this reduced transition probability is discussed in Ref. [36]. Alternative $B(E2)$ values from Coulomb excitation [37–39] and RDDS [39] are also present and clarify the ambiguities related to the 4^+_1 state. A detailed recent study [38] has given two similar $B(E2)$ values for the $4^+_{gsb} \rightarrow 2^+_{gsb}$ transition in ^{98}Ru that fit well with the present calculations. They are noted with green points in the $4^+_{gsb} \rightarrow 2^+_{gsb}$ plot in Fig. 4.

C. Stability of the results against variation of the initial parameters

The variations of the results with small changes of the initial parameters are an important aspect of the calculations. They can be used to estimate the precision of the calculated values.

A few observables were investigated in a more detailed study in the present IBM-1 approach. The energy of the 2^+ state in the quasi-γ band, the staggering index $S(4,3,2)$ and the reduced transition probability for the $E2$ transition from the 2^+ state in the quasi-γ band to the ground state in ^{102}Ru were calculated with varying IBM-1 parameters. Each of ε, κ, κ', and χ was changed in 20 equal steps within $\pm 10\%$ around the values from Fig. 1.

Results of the calculations are shown in Fig. 5. Figures 5(a)–5(d) present the variations of the observables with changes of a single parameter (ε, κ, κ', or χ, respectively). All of the others are fixed to the values from Fig. 1. Figure 5(e) presents the intervals of variations of the observables when all of the IBM-1 parameters are changed within $\pm 10\%$ around the values from Fig. 1.

The calculations show that the energy of the 2^+ state in the quasi-γ band changes mainly with the ε parameter. The variations within $\pm 10\%$ of the other parameters do not have a big impact on $E_{2^+_2}$. The staggering index $S(4,3,2)$ is changing more significantly with variations of κ and κ' rather than ε or χ. The $B(E2; 2^+_2 \rightarrow 0^+_1)$ shows variations in a bit broader interval with strong dependence on ε and κ.

In general, the energy of the 2^+ state in the quasi-γ band and the staggering index $S(4,3,2)$ do not show big deviations when varying slightly the IBM-1 parameters. Their relative change is comparable to the value of $\pm 10\%$ for the variation of the parameters. On the other side, the transition probability for the $E2$ transition from the 2^+ state in the quasi-γ band to the ground state is quite sensitive to the parameter variations. In the present approach it changes within a broad interval, reaching up to 40% deviation of the value corresponding to the parameters from Fig. 1.

IV. THE INTERACTING BOSON-FERMION MODEL-1 (IBFM-1)

The interacting boson-fermion model (IBFM-1) describes odd-A nuclei by coupling of the odd particle to an even-even IBM-1 core [19,20]. Therefore, both collective and single-particle degrees of freedom are taken into account. The model Hamiltonian includes separate bosonic $H_{\rm B}$ and fermionic $H_{\rm F}$ parts and the boson-fermion interaction $V_{\rm BF}$:

$$H = H_{\rm B} + H_{\rm F} + V_{\rm BF}. \tag{9}$$

Here, $H_{\rm B}$ refers to the IBM-1 Hamiltonian used for the description of the even-even core. The fermion part is presented as

$$H_{\rm F} = \sum_j E_j n_j, \tag{10}$$

where E_j denotes the quasiparticle energies of the considered shell-model orbitals.

The third term in the Hamiltonian, the boson-fermion interaction $V_{\rm BF}$, can be described by taking into account several interactions that are sufficient for a phenomenological study of the different properties:

$$V_{\rm BF} = \sum_j A_j n_d n_j + \sum_{jj'} \Gamma_{jj'} [Q \cdot (a^\dagger_j \tilde{a}_{j'})^{(2)}] + \sum_{jj'j''} \Lambda^{j''}_{jj'} : [(d^\dagger \tilde{a}_j)^{(j'')} \times (\tilde{d} a^\dagger_{j'})^{(j'')}]^{(0)}_0. \tag{11}$$

This form of the boson-fermion interaction comprises monopole, quadrupole, and exchange forces [19,40].

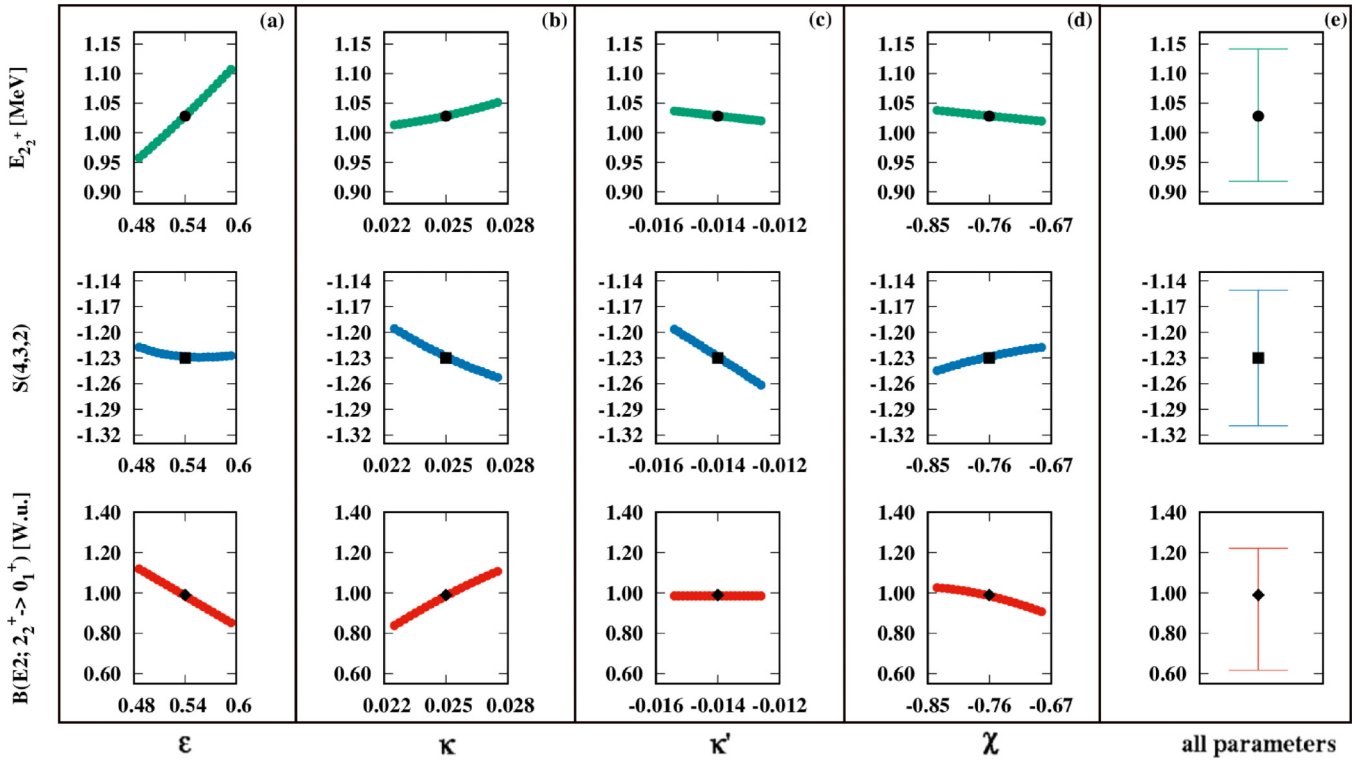

FIG. 5. Changes of the calculated values of $E_{2_2^+}$, $S(4,3,2)$, and $B(E2;2_2^+ \rightarrow 0_1^+)$ in ^{102}Ru with variations of the initial IBM-1 ε, κ, κ', and χ parameters. (a)–(d) Variations when only one of the parameters is changed within $\pm 10\%$ of the values presented in Fig. 1 while the others are kept fixed; (e) intervals of variation when all of the IBM-1 parameters are changed within $\pm 10\%$. The black symbols in all graphs correspond to the results when using the values from Fig. 1. The Y axis in all graphs is significantly expanded to visualize the deviations.

Microscopic considerations can be taken into account to decrease the number of parameters. A common parametrization is given in Ref. [41] and expressed as

$$\begin{aligned} A_j &= A_0, \\ \Gamma_{jj'} &= \Gamma_0(u_j u_{j'} - \upsilon_j \upsilon_{j'})\langle j \| Y^{(2)} \| j' \rangle, \\ \Lambda_{jj'}^{j''} &= -2\sqrt{5}\Lambda_0 \beta_{jj''}\beta_{j''j'}/(2j''+1)^{1/2}(E_j + E_{j''} - \hbar\omega), \end{aligned} \quad (12)$$

where

$$\begin{aligned} \beta_{jj'} &= \langle j \| Y^{(2)} \| j' \rangle (u_j \upsilon_{j'} + \upsilon_j u_{j'}), \\ u_j^2 &= 1 - \upsilon_j^2. \end{aligned} \quad (13)$$

The quantities υ_j^2 are the occupation probabilities of the single-particle orbitals j. The interaction strengths A_0, Λ_0, Γ_0 are free parameters in this approach.

V. ODD-A Ru ISOTOPES

The coupling of the odd neutron to the transitional even-even Ru cores leads to complex structures in the odd nuclei. The high level density at low excitation energies requires a careful analysis of various experimental properties.

The ODDA program package [42] was used in the present IBFM-1 work. The model parameters were obtained after a fit to a number of experimental observables, such as level energies, one-nucleon transfer spectroscopic factors, magnetic dipole and electric quadrupole moments, and $E2$ and $M1$ transition probabilities.

The single-particle energies have a major impact on the calculation of the quasiparticle energies and occupation probabilities and hence on the arrangement of the low-lying parts of the level schemes in the odd-A nuclei [43]. In the present calculations, the $\nu d_{5/2}$, $\nu g_{7/2}$, $\nu s_{1/2}$, $\nu d_{3/2}$, and $\nu h_{11/2}$ orbitals were taken into account because they represent the spherical shell-model configuration between the magic numbers $N = 50$ and $N = 82$. Initial single-particle energies for the orbitals were obtained by using the approach given in Ref. [44].

The single-particle energies were used in a BCS approach to obtain quasiparticle energies and occupation probabilities for the respective orbitals. The pairing strength in the BCS calculation was considered as introducing a pairing gap of $\Delta = 1.5$ MeV. The quasiparticle energies E_j (or, respectively, the single-particle energies) and the occupation probabilities υ_j^2 were adjusted for each isotope in the calculations for better reproduction of the experimental observables. The final values are listed in Table II.

In general, the occupation probabilities and the quasiparticle energies show a smooth behavior. Some more significant changes are observed for the $\nu s_{1/2}$ and $\nu h_{11/2}$ orbitals. The quasiparticle energies for these orbitals decrease away from the shell closure and approach the value for $\nu d_{5/2}$ in ^{105}Ru.

Besides the pure boson part and the single-particle energies all the other parameters in the IBFM-1 Hamiltonian were kept fixed along the isotopic chain. The boson-fermion interaction

TABLE II. Calculated occupation probabilities v_j^2 and quasiparticle energies E_j for the respective orbitals with single-particle energies ε_j used in the present BCS approach for description of $^{99-105}$Ru.

	^{99}Ru			^{101}Ru			^{103}Ru			^{105}Ru		
Orbital	ε_j (MeV)	v_j^2	E_j	ε_j (MeV)	v_j^2	E_j	ε_j (MeV)	v_j^2	E_j	ε_j (MeV)	v_j^2	E_j
$\nu d_{5/2}$	0.0	0.45	1.51	0.0	0.62	1.55	0.0	0.60	1.53	0.0	0.65	1.57
$\nu g_{7/2}$	1.60	0.12	2.31	1.84	0.15	2.09	1.80	0.15	2.13	1.67	0.19	1.93
$\nu s_{1/2}$	1.70	0.11	2.39	1.90	0.14	2.13	1.00	0.29	1.66	0.93	0.35	1.57
$\nu d_{3/2}$	2.90	0.05	3.41	3.00	0.07	3.02	3.00	0.06	3.10	3.30	0.06	3.21
$\nu h_{11/2}$	2.20	0.08	2.79	2.10	0.12	2.28	1.00	0.29	1.66	0.80	0.39	1.54

was described in terms of the free parameters A_0, Λ_0, Γ_0. Best agreement with the available experimental data was found for $A_0 = -0.08$ MeV, $\Gamma_0 = 0.21$ MeV, and $\Lambda_0 = 1.1$ MeV^2, for both positive- and negative-parity states, and all considered nuclei. A value of $\hbar\omega = 1.5$ MeV was used and kept constant in the calculations.

A. Level schemes

The ordering of the low-lying states in the odd-A Ru isotopes placed close to the line of β stability is relatively easy to trace with the mass number, but there are no sufficient data for the heavier isotopes. Ambiguities in the spin and parity assignments are often present. This, along with the increasing number of levels close to the ground state when approaching the neutron midshell, makes the verification of model predictions more difficult.

In the determination of the optimal model parameters we have taken into account different experimental properties of the nuclei: excitation energies, γ-decay characteristics (branching ratios, transition probabilities), electromagnetic moments, and one-nucleon transfer spectroscopic factors. In this section we present a general comparison between the experimental and theoretical level schemes, while in the next sections details of the spectroscopic features are discussed.

1. Positive-parity states

The positive-parity states in the calculations come mainly from the contribution of the $\nu d_{5/2}$, $\nu g_{7/2}$, and $\nu s_{1/2}$ orbitals. A detailed comparison between the theoretical and experimental level schemes has been performed for each isotope. An example of such analysis is shown in Fig. 6 for ^{101}Ru. In this isotope the level scheme up to about 1.2 MeV contains a large number of states, but only few of them have ambiguous spin and parity assignment. A one-to-one correspondence between the theoretical and experimental levels has been attempted. Figure 6 shows a reasonable agreement in both the number of states of each spin and their distribution in energy. For the low-spin states the first three or four levels could be correlated with the calculations. The assignment of an experimental state to a calculated one, as indicated in the figure, was done by comparing different known properties. In some cases only the electromagnetic decay branching ratios were known and it was required that at least the strongest branch is reproduced.

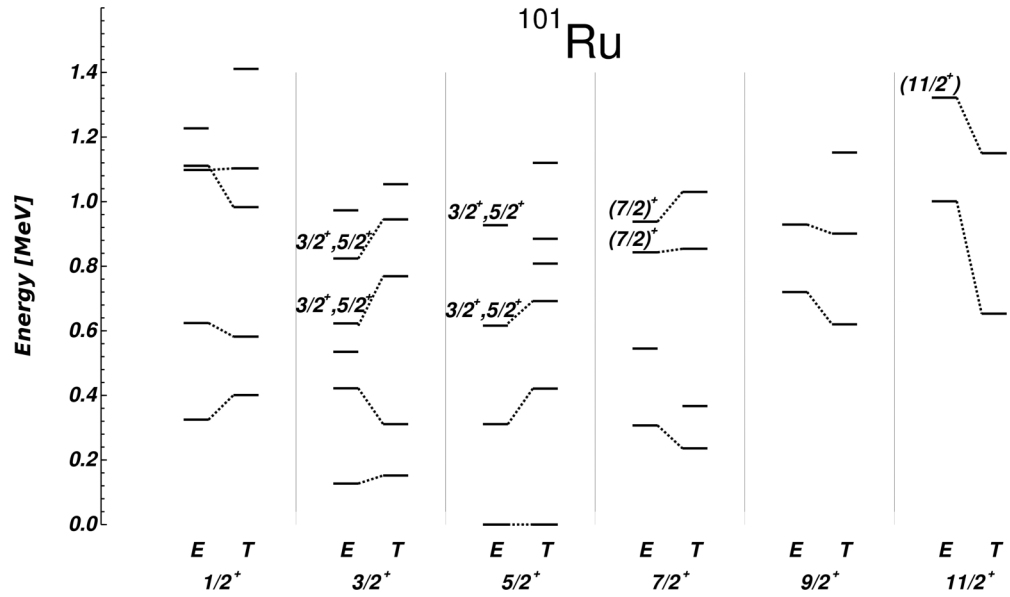

FIG. 6. A comparison between the experimental (E) and theoretical (T) positive-parity states in ^{101}Ru below excitation energy of 1.2 MeV. The E-T associations are based on the electromagnetic decay features and spectroscopic factors from (d,p) reactions. The J^π values are noted for the experimental states where no firm spin and parity assignment is known. The experimental data are taken from Ref. [3].

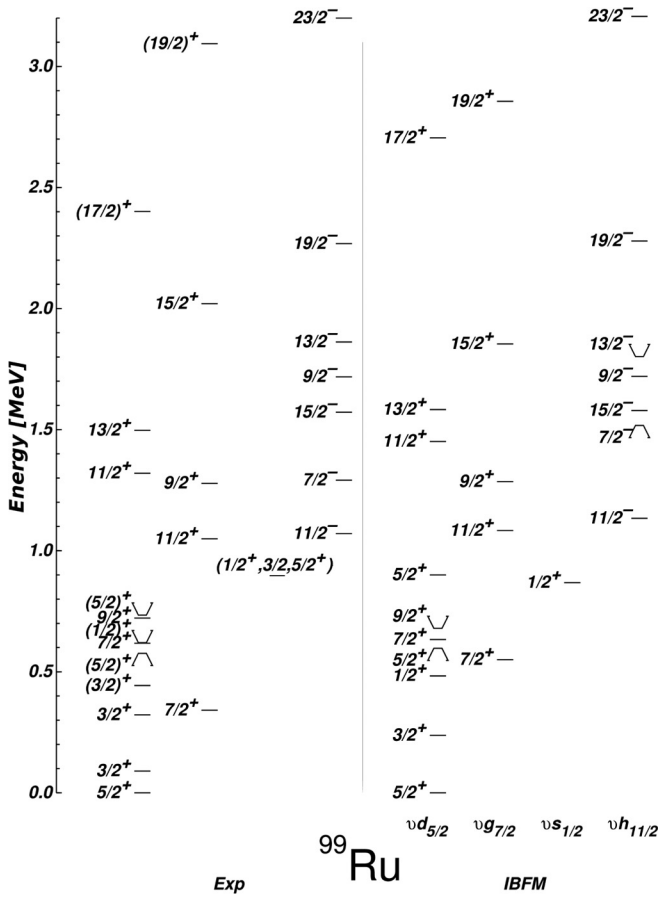

FIG. 7. Experimental partial level scheme of ^{99}Ru compared to the IBFM-1 calculations. The states are arranged according to their theoretical counterparts having a prominent contribution of a particular single-particle orbital. Levels placed above the ground state have a dominant component of $\nu d_{5/2}$. Another positive-parity sequence is governed by $\nu g_{7/2}$. States related to $\nu s_{1/2}$ main contribution are also noted. The negative-parity states appear owing to the unique parity $\nu h_{11/2}$. The experimental data are taken from Ref. [3].

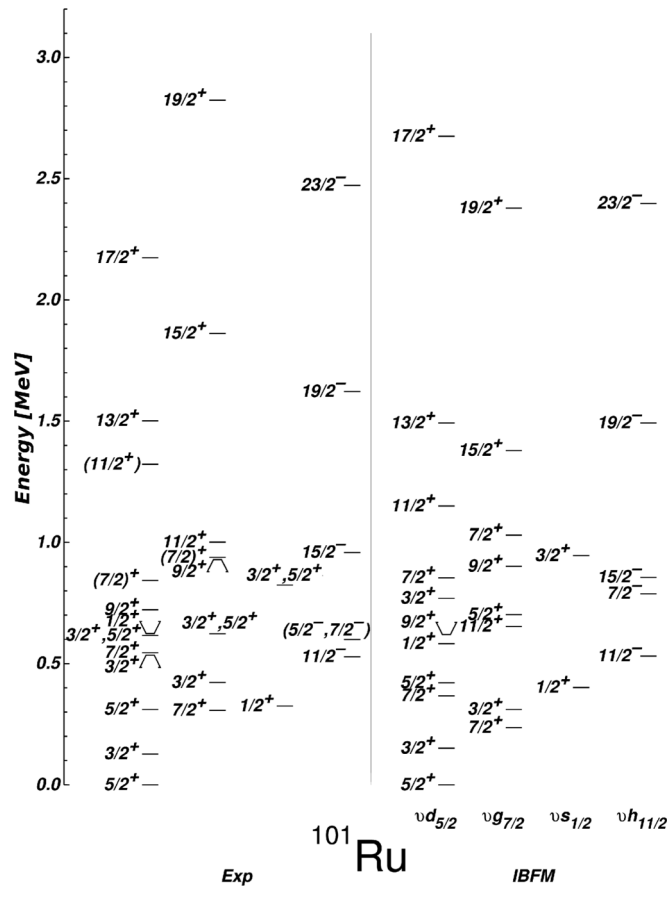

FIG. 8. Same as Fig. 7 but for ^{101}Ru.

A similar one-to-one experiment-theory correlation could be made for ^{99}Ru up to about 1.4 MeV. For the heavier ^{103,105}Ru isotopes this one-to-one correspondence between the experimental and calculated levels has been more difficult to perform owing to the increased level density and many ambiguities in the experimental spin and parity assignments.

In Figs. 7–10 a general comparison between the experimental level schemes and the calculations is shown for all isotopes. Low-spin states with a firmly attributed theoretical counterpart are shown in these figures. In addition, higher-spin states from bandlike structures built on some of the low-lying single-particle excitations are also shown. States with main contribution from $\nu d_{5/2}$ are placed in the ground-state sequences. Bandlike structures based on $\nu g_{7/2}$ are also distinguished. States related to the $\nu s_{1/2}$ orbital are denoted as well.

In all isotopes the first $3/2^+$ and $5/2^+$ states lie close in energy. The ground state of ^{99,101}Ru has $J^\pi = 5/2^+$ that changes to $3/2^+$ in ^{103,105}Ru. In the heavier ^{107,109,111}Ru isotopes $5/2^+$ becomes again the ground state [3]. The configuration of both levels is interpreted as arising from the placement of the odd particle in the $\nu d_{5/2}$ orbital. Some other experimentally observed low-lying $3/2^+$ states are not reproduced in the present IBFM-1 approach.

The predominantly vibrational structure of ^{98}Ru determines the configuration of the low-lying levels in the odd-A ^{99}Ru. In the experimental spectrum a multiplet of states with $J^\pi = 1/2^+$–$9/2^+$ is observed close to the energy of the first phonon excitation in the even core. The levels are grouped in a small energy interval and such a structure is also present in the calculations. These states have a major contribution from the $\nu d_{5/2}$ orbital and are interpreted as arising from one phonon excitations built on the $5/2^+$ ground state. In the heavier isotopes the energy distance between these states increases and the multiplet structure is not so prominent.

A few other higher excitations based on the $\nu d_{5/2}$ orbital are also reproduced. The second $11/2^+$ and the first $13/2^+$ are available to track in ^{99,101,103}Ru and a comparison with the calculations shows a reasonably good agreement. Besides the $13/2^+$ state, which can be interpreted as a two-phonon state coupled to the $\nu d_{5/2}$ orbital, the next core excitation at $17/2^+$ is also observed in ^{99,101}Ru.

Several members of the bandlike structure built on the $7/2^+_1$ state are also well described. A $\Delta J = 2$ sequence emerges on top of this state and a pure $\nu g_{7/2}$ configuration was obtained for the first $7/2^+$, $11/2^+$, $15/2^+$, and $19/2^+$ states. A low-lying $3/2^+$ state with a dominant $\nu g_{7/2}$ contribution also appears

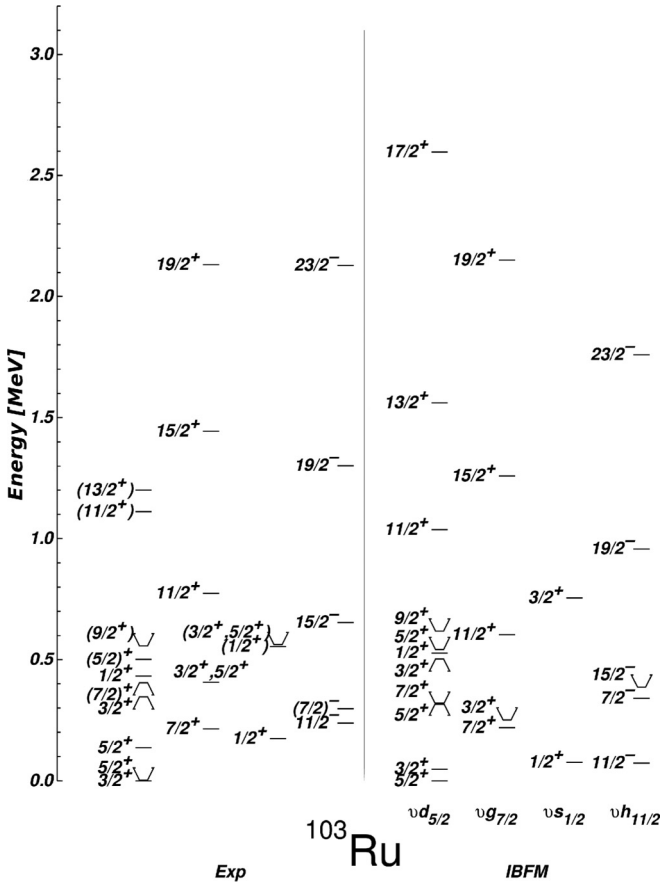

FIG. 9. Same as Fig. 7 but for ^{103}Ru.

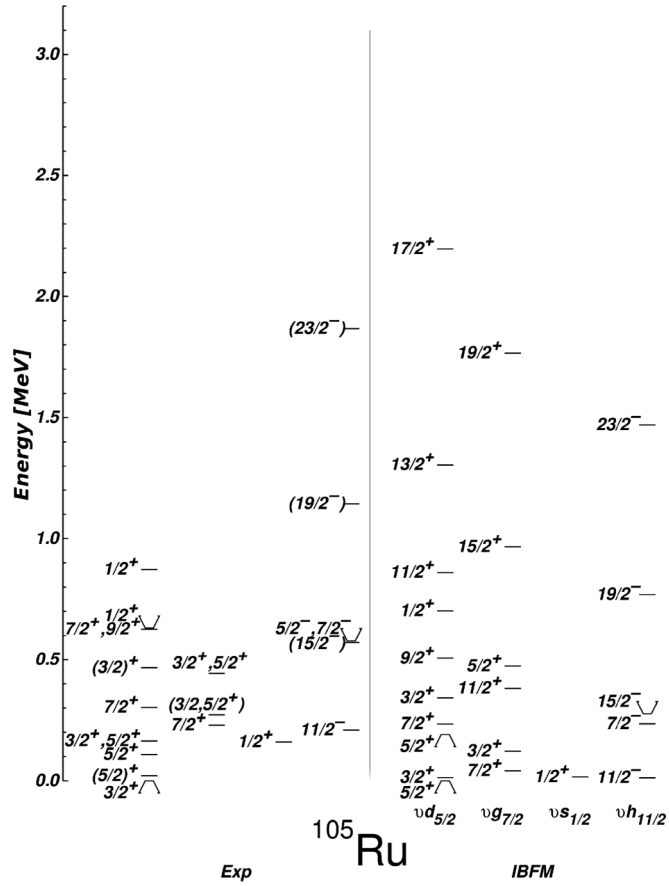

FIG. 10. Same as Fig. 7 but for ^{105}Ru.

close to the $7/2_1^+$ level. It was tentatively attributed to one of the several experimentally observed $3/2^+$ states in this region.

It is interesting to note that states with a dominant $\nu d_{3/2}$ configuration were not obtained at low energies in the present calculations. Several low-lying levels have, at most, 25% contribution from this single-particle orbital. This is probably related to the considerably higher energy of $\nu d_{3/2}$ in comparison to the other orbitals.

States from configurations including the $\nu s_{1/2}$ orbital are present in the calculated level schemes. In all nuclei the $\nu s_{1/2} 1/2^+$ state has to be distinguished from the $1/2^+$ member of the multiplet arising from coupling of the 2^+ core excitation to $\nu d_{5/2}$. Because the structure of these states is not as pure as the $\nu d_{5/2}$- and $\nu g_{7/2}$-based configurations, additional information from comparison between experimental and calculated spectroscopic factors was used. The results are discussed in the next section.

2. *Negative-parity states*

The only neutron orbital with a negative parity in this region is $\nu h_{11/2}$ and it is considered to be responsible for the low-lying negative-parity excitations.

The $11/2^-$ state is the lowest negative-parity state in all Ru isotopes studied in the present work and bands are built on top of it. The energy gaps between the fully aligned members of these bands are typically lower but similar to the energy differences between the excitations in the ground-state bands of the even-even cores. Such a behavior is characteristic for the weak coupling limit and the rotational alignment of moderately deformed nuclei. The placement of the unfavored states can be used to distinguish between these configurations. In the weak coupling limit an almost degenerate multiplet is present while in the rotational alignment scheme the unfavored states are placed at significantly higher excitation energy [1]. The level energies for the unfavored states in ^{99}Ru are placed close to the $15/2^-$ level that represents the fully aligned coupling of the neutron at $\nu h_{11/2}$ to the 2^+ core excitation. This is consistent with the nearly vibrational structure of the ^{98}Ru core. The ordering of the $9/2^-$ and $13/2^-$ states above $15/2^-$ is correctly reproduced. Unfortunately, certain assignments are missing in the heavier odd-mass Ru nuclei and the evolution of the $9/2^-$ and $13/2^-$ states cannot be traced.

The $7/2^-$ state in ^{99}Ru at 1291 keV lies close to the $11/2^-$ bandhead at 1069 keV. An analogous state in ^{103}Ru is the $7/2^-$ at 297 keV, placed near the 238-keV $11/2^-$. In ^{101}Ru such a level is not observed but a $(5/2^-)$ state at 598 keV is present, above the $11/2^-$ state. In this nucleus, the $J^\pi = 7/2^-$ assignment is not excluded and is preferred in the analysis of (d,p) reactions [45]. Such an assignment fits the state better within the systematics of the neighboring nuclei. Present calculations suggest that the $7/2^-$ lie close in energy to $15/2^-$. Thus, the IBFM-1 $7/2^-$ energy is overestimated,

but nevertheless it is clear that this state is part of the negative-parity multiplets.

The $7/2^-$ state in ^{99}Ru was previously studied in the framework of particle-core coupling. A configuration of antialigned angular momenta of a 2^+ core excitation and the neutron placed at the $\nu h_{11/2}$ orbital was ascribed. The significantly low experimental energy was understood as an effect of the Coriolis interaction [46,47]. Such an explanation is consistent with the present IBFM-1 results. An important note is that a transition between the $7/2^-$ and $11/2^-$ states is not observed; the $7/2^-$ state decays only via a pure $E1$ transition to the $5/2^+$ ground state.

Because the negative-parity bands have a similar structure in all odd-A Ru isotopes in this region, the same antialigned angular momenta configuration is suggested for the $7/2^-$ states in ^{101,103}Ru.

B. One-nucleon transfer reactions

The reactions with a transfer of a single nucleon can be used as an important tool to investigate the structure of nuclei. The single-particle component of the wave function of the states can be examined on the basis of the spectroscopic strengths for such reactions.

The odd-A Ru isotopes were studied in the past in (d,p) reactions and experimental data are available for most of them [3]. Here a comparison with IBFM-1 calculations is performed for some of the low-lying excited states.

The operator for one-nucleon transfer reactions between nuclei with equal number of bosons has the form [40,41]

$$c_j^\dagger = \Bigg[u_j a_j^\dagger - \sum_{j'} \frac{\upsilon_j}{\sqrt{N_\pi}} \sqrt{\frac{10}{2j+1}} \frac{N_\pi}{N} \times \beta_{j'j}(K_\beta)^{-1} s^\dagger (\tilde{d} a_{j'}^\dagger)^{(j)} \Bigg] \Big/ K_j, \tag{14}$$

with $\beta_{jj'}$ related to $\langle j||Y_2||j'\rangle$ as expressed in Eq. (13) and

$$K_\beta^2 = \sum_{jj'} \beta_{jj'}^2. \tag{15}$$

The normalization coefficient K_j is defined by the condition

$$\sum_{\text{odd}} \langle \text{odd}(A+1)|c_j^\dagger|\text{even}(A)_{\text{gs}}\rangle^2 = (2j+1)u_j^2, \tag{16}$$

with summation over all levels of a given angular momentum in the odd nucleus.

Spectroscopic factors are calculated using the relation

$$S = \langle \text{odd}(A+1) \Big\| c_j^\dagger \Big\| \text{even}(A)_{\text{gs}}\rangle^2, \tag{17}$$

with the proper normalization applied to obey the spectroscopic factor sum rules.

To trace the evolution of the single-particle states with neutron number, experimental spectroscopic factors data are used. Data for ^{99}Ru do not exist but are available for ^{101,103,105}Ru. A comparison between the experimental and calculated spectroscopic factors is presented in Table III.

The C^2S' values refer to the relation

$$C^2S' = C^2 \frac{2J_f+1}{2J_i+1} S = C^2(2J_f+1)S, \tag{18}$$

where C^2 denotes the squared isospin Clebsch-Gordan coefficient for single-nucleon transfer. The value of C^2 for neutron stripping is 1 [48].

The comparison between the experimental data and calculations shows a reasonable agreement for the C^2S' values. The spectroscopic factors for the $11/2^-$ states are overestimated, especially in the heavier isotopes. The values for the first $5/2^+$ states decrease with increasing of the number of neutrons and are comparable with the experimental data. The same is valid for the first $7/2^+$ states, except that the sharp decrease of C^2S' in ^{103,105}Ru is not well reproduced.

Special attention should be paid to the $3/2^+$ ground state in ^{103}Ru, which has a spectroscopic factor much larger than the one obtained in the calculations. Difficulties in studying this state arise from the close-lying $5/2^+$, which is just 2.81 keV above the ground state. The value of $C^2S' = 1.44$ is based on a (d,p) reaction study in which a major population of the ground state was associated with the lowest-lying $\ell = 2$ transfer [49]. Within the measured energy difference of 1.0 ± 1.2 keV this spectroscopic factor was assigned to the $3/2^+$ state and adopted in Evaluated Nuclear Structure Data File (ENSDF) [3]. A later work states that if the lowest-lying $\ell = 2$ transfer is attributed to the ground state, a shift of -3.3 ± 0.2 keV is present for about 20 strong transitions [50]. Thus, a major population of the first excited $5/2^+$ state is suggested and the large spectroscopic factor is assigned to it. This value is also adopted in ENSDF [3]. In the present calculations, a large spectroscopic factor for the $5/2^+$ level is obtained, while the one for the $3/2^+$ state is small. This is in agreement with Ref. [50].

The $1/2^+$ states also represent a challenge for the model interpretations because the configurations based on the $\nu d_{5/2}$ and $\nu s_{1/2}$ orbitals have to be distinguished. The experimental data for the $1/2^+$ spectroscopic factors give essential information in this respect. A comparison between the experimental and calculated energies of the $1/2^+$ states in the Ru isotopes is shown in Fig. 11. The values for the spectroscopic factors are also denoted. The reproduction of the $1/2^+$ spectroscopic factors validates the predicted contributions of the $\nu s_{1/2}$ orbital to the wave functions.

One $1/2^+$ state with a large C^2S' appears in ^{97}Ru at 908.29 keV, while a firm assignment for another low-lying $1/2^+$ state is not present. In ^{99}Ru data for the spectroscopic factors are not available but within the IBFM calculations a $1/2^+$ state with a dominant $\nu s_{1/2}$ component appears at 868 keV. It can be possibly related to the experimentally known ($1/2^+$, 3/2, $5/2^+$) state at 896.85 keV.

C. Electromagnetic properties

The operator for $E2$ transitions in IBFM-1 has the form

$$T(E2) = e_B[(s^\dagger \tilde{d} + d^\dagger s)^{(2)} + \chi(d^\dagger \tilde{d})^{(2)}] - e_F \sum_{jj'} (u_j u_{j'} - \upsilon_j \upsilon_{j'}) \langle j \| Y^{(2)} \| j' \rangle \times [(a_j^\dagger \tilde{a}_{j'})^{(2)} + \text{c.c.}], \tag{19}$$

TABLE III. Experimental and calculated spectroscopic factors for states in the odd-A Ru isotopes populated in (d,p) reactions.

Isotope	E_{level}[a] (keV)	ℓ	J^π[a]	$C^2S'_{exp}$	$C^2S'_{IBFM}$	Isotope	E_{level}[a] (keV)	ℓ	J^π[a]	$C^2S'_{exp}$	$C^2S'_{IBFM}$
^{99}Ru	0.0		$5/2^+$		3.11	^{103}Ru	0.0	2[e]	$3/2^+$	1.44[e]	0.010
^{99}Ru	89.57		$3/2^+$		0.008	^{103}Ru	2.81	2[f]	$5/2^+$	1.35[f]	2.09
^{99}Ru	340.90		$7/2^+$		2.97	^{103}Ru	136.079	2[f]	$5/2^+$	0.012[f]	0.12
^{99}Ru	575.83		$(5/2)^+$		0.03	^{103}Ru	174.26	0[f]	$1/2^+$	0.75[f]	1.13
^{99}Ru	734.09		$(5/2)^+$		0.005	^{103}Ru	213.56	4[f]	$7/2^+$	1.80[f]	3.69
^{99}Ru	896.85		$(1/2^+,3/2,5/2)^+$		0.85[b]	^{103}Ru	238.2	5[f]	$11/2^-$	3.2[f]	7.04
^{99}Ru	1069.88		$11/2^-$		8.86	^{103}Ru	346.38	2[f]	$3/2^+$	0.06[f]	0.005
						^{103}Ru	404.15		$7/2^+$		0.006
						^{103}Ru	432.06	0[f]	$1/2^+$	0.027[f]	0.047
						^{103}Ru	501.15	2[f]	$(5/2)^+$	0.032[f]	0.039
^{101}Ru	0.0	2[c]	$5/2^+$	2.10[c]	1.97	^{105}Ru	0.0	2[g]	$3/2^+$	0.009[g]	0.13
^{101}Ru	127.229	2[c]	$3/2^+$	0.067[c]	0.014	^{105}Ru	20.610	2[g]	$(5/2)^+$	1.54[g]	1.55
^{101}Ru	306.858	4[c]	$7/2^+$	5.3[c]	4.12	^{105}Ru	107.937	2[g]	$5/2^+$	0.07[g]	0.28
^{101}Ru	311.368		$5/2^+$		0.07	^{105}Ru	159.518	0[g]	$1/2^+$	0.74[g]	0.90
^{101}Ru	325.23	0[c]	$1/2^+$	0.96[c]	1.12	^{105}Ru	208.6	5[g]	$11/2^-$	2.7[g]	6.06
^{101}Ru	422.22	2[c]	$3/2^+$	0.15[c]	0.66	^{105}Ru	229.48	4[g]	$7/2^+$	0.75[g]	3.42
^{101}Ru	527.56	5[c]	$11/2^-$	5.8[c]	7.68	^{105}Ru	272.722		$(3/2,5/2^+)$		0.31[d]
^{101}Ru	545.115		$7/2^+$		0.003	^{105}Ru	301.68	4[g]	$7/2^+$	0.24[g]	0.03
^{101}Ru	623.59	0[c]	$1/2^+$	0.063[c]	0.021	^{105}Ru	631.27	0[g]	$1/2^+$	0.06[g]	0.07
^{101}Ru	824	2[c]	$3/2^+$, $5/2^+$	0.40[c],[d]	0.31[d]						
^{101}Ru	1098	0[c]	$1/2^+$	0.028[c]	0.10						
^{101}Ru	1111	0[c]	$1/2^+$	0.17[c]	0.28						

[a]Data from Ref. [3].
[b]If assigned $J^\pi = 1/2^+$ on the basis of the IBFM calculations.
[c]Data from Ref. [45].
[d]If assigned $J^\pi = 3/2^+$ on the basis of the IBFM calculations.
[e]Data from Ref. [49].
[f]Data from Ref. [50].
[g]Data from Ref. [51].

where the parameters e_B and e_F stand for the effective boson and effective fermion charges, respectively.

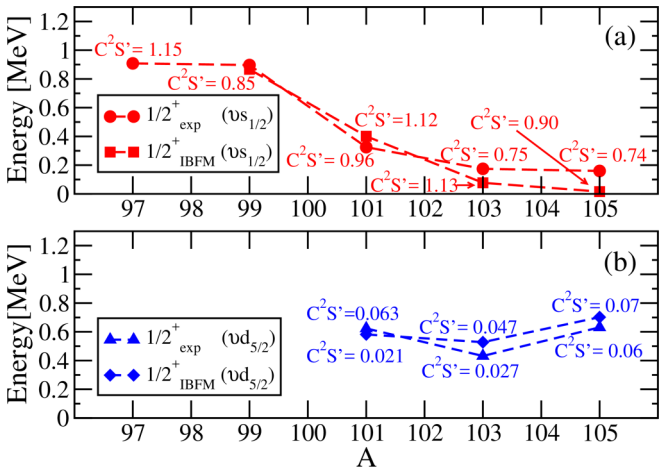

FIG. 11. Experimental and calculated $1/2^+$ states in the odd $^{97-105}$Ru isotopes; the arrangement is based on the dominant component in the wave function. (a) Levels related to configurations with main contribution from $\nu s_{1/2}$; (b) states with large $\nu d_{5/2}$ component. Experimental and calculated spectroscopic factors are denoted where available. The experimental data are taken from Ref. [3].

The simplest operator for $M1$ transitions is written as

$$T(M1) = \sqrt{\frac{90}{4\pi}} g_d (d^\dagger \tilde{d})^{(1)} - g_F \sum_{jj'} (u_j u_{j'} + \upsilon_j \upsilon_{j'}) \cdot \times \langle j \| g_l l + g_s s \| j' \rangle [(a_j^\dagger \tilde{a}_{j'})^{(1)} + \text{c.c.}], \quad (20)$$

where g_d is an effective d-boson g factor and g_F is a fermionic g factor that normalizes the g_l and g_s values [41]. The use of a more complex operator for $M1$ transitions can result in a better reproduction of the experimental data but such an approach introduces additional free parameters [52]. The aim of the present calculations is to use a small number of free parameters and hence complicated forms of the $M1$ transition operator were avoided.

The effective boson charge in the operator for $E2$ transitions was set to the same value used in the calculations for the even Ru nuclei. The effective fermion charge was assumed to be of the same magnitude ($e_F = e_B$). A value of $g_l = 0$ was used for the $M1$ transitions given that the odd particle is a neutron. The effective boson g-factor g_d was set to 0.8 μ_N according to the magnetic moments of the 2^+ states in neighboring even Ru isotopes [53]. The g_s factor was fixed to -2.68 μ_N, indicating a quenching to 70% of the free neutron value.

TABLE IV. Experimental and calculated magnetic dipole and electric quadrupole moments. The experimental data are taken from Ref. [53], unless otherwise noted.

Isotope	E_{level}[a] (keV)	J^{π}[a]	μ_{exp} (μ_N)	μ_{IBFM} (μ_N)	Q_{exp} (b)	Q_{IBFM} (eb)
^{99}Ru	0	$5/2^+$	−0.641 (5)	−1.282	+0.079(4)	+0.086
^{99}Ru	89.57	$3/2^+$	−0.284(6)	−0.380	+0.231(12)	+0.232
^{101}Ru	0	$5/2^+$	−0.719 (6)	−1.189	+0.46 (2)	+0.45
^{101}Ru	127.229	$3/2^+$	−0.210 (5)	−0.193		
^{103}Ru	0	$3/2^+$	0.200 (7)	−0.040	(+)0.62 (2)	+0.27
^{105}Ru	0	$3/2^+$	(−)0.32 (+8/−20)	+0.126		

[a]Data from Ref. [3].

1. Electromagnetic moments

Magnetic dipole and electric quadrupole moments were calculated within the IBFM-1 approach. Experimental data are available for the first $5/2^+$ and $3/2^+$ states in some of the studied isotopes. A comparison with the theoretical values is presented in Table IV.

A good agreement between the IBFM-1 results and the experimental data is obtained. The sign of the moments is reproduced everywhere, except for the magnetic dipole moment of the $3/2^+$ state in ^{103}Ru where the calculated value is negative but close to zero. The electric quadrupole moments in ^{99,101}Ru are described very well but unfortunately experimental data are not available for other states besides the first $3/2^+$ and $5/2^+$.

2. Transition probabilities

Model predictions for transitions within and between the bandlike structures built on $\nu d_{5/2}$ and $\nu g_{7/2}$ are of particular interest because these two orbitals have dominant contribution to the wave functions of the low-lying states. Experimental data for such $M1$ and $E2$ transitions are available in ^{99,101}Ru and $B(E2)$ and $B(M1)$ values are compared to the IBFM-1 calculations in Table V. The reduced transition probabilities are calculated using the relations from Eqs. (19), (20), and (8). Calculated and experimental branching ratios are also denoted. They were used for a more comprehensive interpretation of the level schemes. A detailed comparison between the experimental and theoretical positive-parity states in ^{101}Ru below 1.2 MeV based on the branching ratios and spectroscopic factors from (d,p) reactions has been presented in Fig. 6.

The states within each of the $\nu d_{5/2}$ and $\nu g_{7/2}$ based bandlike structures are connected via strong $E2$ transitions and their behavior is reproduced well by the calculations. The $B(E2)$ values are comparable to the magnitudes of the transition strengths in the ground-state bands of ^{98}Ru and ^{100}Ru.

More difficulties are encountered in the description of transitions connecting states with different dominant orbital contribution. Several $M1+E2$ mixed transitions that connect the two configurations were observed in ^{99}Ru and ^{101}Ru. Most of the transitions of interest have experimentally known small mixing ratios with large uncertainties [3]. In this case any small change in δ can affect significantly the experimental $B(E2)$ values. Thus, often a comparison with the theoretical $E2$ transition probabilities does not provide a reliable basis for interpretation but the $M1$ components must be studied more carefully.

Many of the calculated $M1$ strengths deviate from the experimental data within an order of magnitude. This is not uncommon for $M1$ transitions calculated in the IBFM, especially with the simplest $M1$ transition operator as used here. However, even without any comparison to the model predictions the experimental $B(M1)$ values alone give some important information. All experimental $M1$ strengths are weaker than the single-particle estimations. The transition between the lowest-lying $7/2^+$ and $5/2^+$ states is of a particular interest because the experimental and calculated spectroscopic factors and the IBFM-1 wave functions show very pure single-particle configurations for these states. The transition between the $\nu d_{5/2}$ and $\nu g_{7/2}$ orbitals can be understood well within the systematics of the $M1$ transitions. In the pure shell model the magnetic dipole operator does not lead to changes in the angular momentum and the initial and final states must not differ in orbital angular momentum. Hence, the $M1$ transitions that do not satisfy this rule are called ℓ-forbidden and are delayed by approximately two orders of magnitude [55]. Indeed, the $7/2_1^+ \rightarrow 5/2_1^+$ transitions in ^{99,101}Ru connect states with different orbital angular momentum and the $B(M1)$ values are of the order of the typical ℓ-forbidden $M1$ transition values. Such configurations are common in neighboring nuclei in the $A \sim 100$ region. Therefore, the interpretation of the $7/2_1^+$ and $5/2_1^+$ states in the Ru isotopes is consistent with the systematics.

VI. CONCLUSION

The structure of the low-lying states in the $A \approx 100$ Ru isotopes was studied using the IBM-1 and IBFM-1 models. The transition from nearly vibrational to γ-soft behavior in this part of the isotopic chain was previously observed in the even Ru nuclei [10]. Here a coupling of the odd neutron to the calculated transitional cores was applied for the odd $^{99-105}$Ru. The structure of the low-lying states in these isotopes was studied using the same boson-fermion interaction for both the positive- and negative-parity neutron orbitals between the magic numbers $N = 50$ and $N = 82$. Calculated level energies, transition probabilities, branching ratios, one-nucleon transfer spectroscopic factors, magnetic dipole, and electric quadrupole moments were compared to

TABLE V. A comparison between the experimental and calculated $B(M1)$ and $B(E2)$ values and branching ratios in ^{99,101}Ru. The experimental data are taken from the adopted levels and γ's in ENSDF [3], unless otherwise noted.

Isotope	E_{level} (keV)	J_i^π	E_γ (keV)	J_f^π	$B(M1)_{\text{exp}}$ (W.u.)	$B(E2)_{\text{exp}}$ (W.u.)	$B(M1)_{\text{IBFM}}$ (W.u.)	$B(E2)_{\text{IBFM}}$ (W.u.)	I_{exp}	I_{IBFM}
^{99}Ru	89.57	$3/2^+$	89.50	$5/2^+$	0.000 175 (4)	50.1 (10)	0.000 169	31.0	100	100
^{99}Ru	340.90	$7/2^+$	251.0	$3/2^+$		3.0[a] (12)		2.0	0.7	2.5
			340.81	$5/2^+$	0.011[a] (5)	0.036[a] (23)	0.0008	11	100	100
^{99}Ru	575.83	$(5/2)_2^+$	486.19	$3/2^+$	0.11 (3)	0.18 (+53/ − 18)	0.57	3.78	100	100
			575.75	$5/2^+$	0.035 (10)	11 (5)	0.001	23	58.5	2.7
^{99}Ru	617.89	$7/2_2^+$	528.36	$3/2^+$		120 (70)		3	22	8.3
			617.89	$5/2^+$	0.09 (6)	23 (18)	0.002	15	100	100
^{99}Ru	719.87	$9/2^+$	379.07	$7/2^+$	0.0045 (8)	3 (+4/ − 3)	0.052	6.9	2.9	54.5
			719.81	$5/2^+$		46 (6)		26	100	100
^{99}Ru	1048.50	$11/2^+$	328.57	$9/2^+$	0.011 (7)	2.9 (17)	0.0004	0.1	9.5	0.4
			707.56	$7/2^+$		23 (13)		19	100	100
^{99}Ru	1497.06	$13/2^+$	777.25	$9/2^+$		110 (60)		38	100	100
^{99}Ru	2020.29	$15/2^+$	971.95	$11/2^+$		61 (25)		40	100	100
^{99}Ru	2400.88	$(17/2)^+$	903.91	$13/2^+$		50 (30)		39	100	100
^{99}Ru	3094.45	$(19/2)^+$	1074.14	$15/2^+$		35 (+14/ − 29)		40	100	100
^{99}Ru	3200.19	$23/2^-$	931.89	$19/2^-$		70 (+12/ − 24)		44	100	100
^{101}Ru	127.229	$3/2^+$	127.226	$5/2^+$	0.01598 (11)	19.9 (24)	0.053	31.4	100	100
^{101}Ru	306.858	$7/2^+$	179.636	$3/2^+$		13 (4)		2	0.7	1.1
			306.857	$5/2^+$	0.014 (4)	1.4 (+15/ − 4)	0.001	0.8	100	100
^{101}Ru	311.368	$5/2_2^+$	184.10	$3/2^+$	>0.021		0.46		100	100
			311.38	$5/2^+$	>0.000 53		0.0077		12.3	10.7
^{101}Ru	545.115	$7/2_2^+$	233.72	$5/2_2^+$	0.043 (10)		0.28		4.2	54.2
			238.25	$7/2^+$	0.048 (11)		0.021		4.7	4.2
			417.86	$3/2^+$		4.4 (20)		6.5	0.1	1.4
			545.117	$5/2^+$	0.042 (10)	130 (30)	0.024	52	100	100
^{101}Ru	720.02	$9/2^+$	720.02	$5/2^+$		40 (10)		31	100	100
^{101}Ru	1500.9	$13/2^+$	780.9	$9/2^+$		120 (40)		48	100	100
^{101}Ru	1862.4	$15/2^+$	861.2	$11/2^+$		< 25		57	100	100
^{101}Ru	2173.9	$17/2^+$	673.0	$13/2^+$		< 110		29	100	100

[a]Data from Ref. [54].

experimental data. ^{99}Ru was interpreted as a nearly vibrational core coupled to the odd neutron and the transition towards a structure of a γ-soft core plus a particle is observed in the heavier isotopes. Most of the positive-parity low-lying states were described by configurations involving the $\nu d_{5/2}$ and $\nu g_{7/2}$ orbitals, while the negative-parity states were attributed to $\nu h_{11/2}$. The role of the $\nu s_{1/2}$ orbital was also recognized, mostly using spectroscopic factors data from (d,p) reactions.

In general, the systematics of the observable experimental and calculated properties show that the studied Ru isotopes are placed in a region where deformation arises and a complex interplay between the single-particle and collective degrees of freedom is present.

ACKNOWLEDGMENTS

S.K. would like to thank R. F. Casten, P. Van Isacker, S. Pascu, M. K. Smith, and P. Petkov for their suggestions and recommendations related to this work. S.K. is grateful to the organizers of the Training in Advanced Low Energy Nuclear Theory (TALENT), Course 5: Theory for exploring nuclear structure experiments, GANIL, France, 2014, and to all lecturers and participants in the school for the constructive and interesting discussions. This project is supported by the Bulgarian National Science Fund under Contract No. DFNI-E02/6 and Romanian UEFISCDI Project No. PN-II-ID-PCE-2011-3-0140.

[1] R. F. Casten, *Nuclear Structure From a Simple Perspective*, 2nd ed. (Oxford University Press, Oxford, UK, 2000).
[2] H. G. Börner, R. F. Casten, M. Jentschel, P. Mutti, W. Urban, and N. V. Zamfir, Phys. Rev. C **84**, 044326 (2011).
[3] NNDC data base, www.nndc.bnl.gov.
[4] S. Lalkovski and N. Minkov, J. Phys. G: Nucl. Part. Phys. **31**, 427 (2005).
[5] J. Srebrny *et al.*, Nucl. Phys. A **766**, 25 (2006).
[6] J. A. Shannon *et al.*, Phys. Lett. B **336**, 136 (1994).
[7] F. Iachello and A. Arima, Phys. Lett. B **53**, 309 (1974).
[8] A. Arima and F. Iachello, Phys. Rev. Lett. **35**, 1069 (1975).
[9] P. Van Isacker and G. Puddu, Nucl. Phys. A **348**, 125 (1980).
[10] J. Stachel, P. Van Isacker, and K. Heyde, Phys. Rev. C **25**, 650 (1982).

[11] R. F. Casten, W. Frank, and P. von Brentano, Nucl. Phys. A **444**, 133 (1985).
[12] D. Bucurescu, G. Căta, D. Cutoiu, G. Constantinescu, M. Ivaşcu, and N. V. Zamfir, Z. Phys. A **324**, 387 (1986).
[13] A. Frank, P. Van Isacker, and D. D. Warner, Phys. Lett. B **197**, 474 (1987).
[14] A. Giannatiempo, A. Nannini, P. Sona, and D. Cutoiu, Phys. Rev. C **52**, 2969 (1995).
[15] A. Frank, C. E. Alonso, and J. M. Arias, Phys. Rev. C **65**, 014301 (2001).
[16] J. Kotila, J. Suhonen, and D. S. Delion, Phys. Rev. C **68**, 054322 (2003).
[17] I. Stefanescu *et al.*, Nucl. Phys. A **789**, 125 (2007).
[18] S. Lalkovski *et al.*, Phys. Rev. C **89**, 064312 (2014).
[19] F. Iachello and O. Scholten, Phys. Rev. Lett. **43**, 679 (1979).
[20] F. Iachello and P. van Isacker, *The Interacting Boson-Fermion Model* (Cambridge University Press, Cambridge, UK, 1991).
[21] E. H. du Marchie van Voorthuysen, M. J. A. de Voigt, N. Blasi, and J. F. W. Jansen, Nucl. Phys. A **355**, 93 (1981).
[22] G. Maino, A. Ventura, A. M. Bizzeti-Sona, and P. Blasi, Z. Phys. A **340**, 241 (1991).
[23] J. M. Arias, C. E. Alonso, and M. Losano, Nucl. Phys. A **466**, 295 (1987).
[24] R. F. Casten and D. D. Warner, Rev. Mod. Phys. **60**, 389 (1988).
[25] W. Pfeifer, *An Introduction to the Interacting Boson Model of the Atomic Nucleus* (vdf-Hochschulverlag AG an der ETH Zürich, Zürich, 1998).
[26] F. Iachello and A. Arima, *The Interacting Boson Model* (Cambridge University Press, Cambridge, UK, 1987).
[27] D. D. Warner and R. F. Casten, Phys. Rev. C **28**, 1798 (1983).
[28] W. Greiner and J. A. Maruhn, *Nuclear Models* (Springer-Verlag, Berlin, 1996).
[29] J. Jolie, R. F. Casten, P. von Brentano, and V. Werner, Phys. Rev. Lett. **87**, 162501 (2001).
[30] P. O. Lipas, P. Toivonen, and D. D. Warner, Phys. Lett. B **155**, 295 (1985).
[31] O. Scholten, program package PHINT, internal report KVI-63, Kernfysisch Versneller Instituut, Groningen, The Netherlands.
[32] L. Wilets and M. Jean, Phys. Rev. **102**, 788 (1956).
[33] M. Sakai and A. C. Rester, At. Data Nucl. Data Tables **20**, 441 (1977).
[34] D. J. Rowe and J. L. Wood, *Fundamentals of Nuclear Models: Foundational Models* (World Scientific, Singapore, 2010).
[35] B. Kharraja *et al.*, Phys. Rev. C **61**, 024301 (1999).
[36] R. B. Cakirli, R. F. Casten, J. Jolie, and N. Warr, Phys. Rev. C **70**, 047302 (2004).
[37] S. Landsberger, R. Lecomte, P. Paradis, and S. Monaro, Phys. Rev. C **21**, 588 (1980).
[38] E. Williams *et al.*, Phys. Rev. C **74**, 024302 (2006).
[39] D. Radeck *et al.*, Phys. Rev. C **85**, 014301 (2012).
[40] J. Jolie, P. van Isacker, K. Heyde, J. Moreau, G. van Landeghem, M. Waroquier, and O. Scholten, Nucl. Phys. A **438**, 15 (1985).
[41] O. Scholten, Ph.D. thesis, University of Groningen, 1980.
[42] O. Scholten, program package ODDA, KVI Internal Report No. 255, 1980.
[43] D. Bucurescu, G. Cata-Danil, N. V. Zamfir, A. Gizon, and J. Gizon, Phys. Rev. C **43**, 2610 (1991).
[44] B. S. Reehal and R. A. Sorensen, Phys. Rev. C **2**, 819 (1970).
[45] J. L. M. Duarte, L. B. Horodynski-Matsushigue, T. Borello-Lewin, and O. Dietzsch, Phys. Rev. C **38**, 664 (1988).
[46] C. S. Whisnant, R. H. Castain, F. A. Rickey, and P. C. Simms, Phys. Rev. Lett. **50**, 724 (1983).
[47] C. S. Whisnant, K. D. Carnes, R. H. Castain, F. A. Rickey, G. S. Samudra, and P. C. Simms, Phys. Rev. C **34**, 443 (1986).
[48] M. R. Bhat, Procedures Manual for the Evaluated Nuclear Structure Data File, BNL-NCS-40503 Informal Report, 1987.
[49] G. P. A. Berg *et al.*, Nucl. Phys. A **379**, 93 (1982).
[50] M. D. L. Barbosa, T. Borello-Lewin, L. B. Horodynski-Matsushigue, J. L. M. Duarte, G. M. Ukita, and L. C. Gomes, Phys. Rev. C **58**, 2689 (1998).
[51] P. Maier-Komor, P. Gläissel, E. Huenges, H. Rösler, H. J. Scheerer, H. K. Vonach, and H. Baier, Z. Phys. A **278**, 327 (1976).
[52] M. Ivaşcu, N. Mărginean, D. Bucurescu, I. Căta-Danil, C. A. Ur, and Yu. N. Lobach, Phys. Rev. C **60**, 024302 (1999).
[53] N. J. Stone, At. Data Nucl. Data Tables **90**, 75 (2005).
[54] S. Kisyov *et al.*, Bulg. J. Phys. **42**, 583 (2015).
[55] A. Arima, H. Horie, and M. Sano, Prog. Theor. Phys. **17**, 567 (1957).